

Magnetic interactions, bonding, and motion of positive muons in magnetite

C. Boekema and R. L. Lichti

Texas Tech University, Lubbock, Texas 79409

V. A. M. Brabers

University of Technology, Eindhoven, 5600 MB Eindhoven, The Netherlands

A. B. Denison

University of Wyoming, Laramie, Wyoming 82071

D. W. Cooke, R. H. Heffner, R. L. Hutson, M. Leon, and M. E. Schillaci

Los Alamos National Laboratory, Los Alamos, New Mexico 87545

(Received 2 August 1984)

Positive-muon behavior in magnetite is investigated by the muon-spin-rotation technique. The observed muon relaxation rate in zero applied field, in conjunction with the measured local field, allows us to separate muon-motion effects from phase transitions associated with magnetite. The local magnetic field is observed to be 4.02 kOe directed along the $\langle 111 \rangle$ axis, the easy axis of magnetization. Possible origins of this field are discussed in terms which include local muon diffusion and a supertransfer hyperfine interaction resulting from muon-oxygen bonding. An anomaly in the muon hyperfine interactions is observed at 247 K.

I. INTRODUCTION

The positive-muon spin-rotation (μ SR) technique has been shown to be an excellent method for investigating static and dynamic local magnetic fields in solids.¹⁻³ Owing to its positive charge, the muon usually resides at an interstitial site in a crystal and consequently probes those regions normally inaccessible to other more conventional techniques (magnetic resonance, Mössbauer, etc.). Among the numerous systems investigated by μ SR, some recent attention has been devoted to magnetic oxides.⁴⁻⁸ Of special interest in these studies has been the determination of the origin, magnitude, and direction of the local field experienced by the muon; a nontrivial task since the μ^+ stopping site was initially unknown. Basic conclusions drawn from these studies were that (1) in a certain temperature regime μ^+ diffusion accounted for the measured relaxation rate, whereas (2) at other temperatures μ^+ localization occurred and, in fact, could be attributed to the formation of a muon-oxygen bond (analogous to a hydrogen bond). These intriguing results coupled with a basic desire to achieve a better understanding of μ^+ behavior in magnetic oxides have led us to investigate magnetite (Fe_3O_4) by utilizing the μ SR technique.

Magnetite is a ferrimagnetic oxide ($T_{FN} = 858$ K) that undergoes a metal-to-insulator transition at the well-known Verwey⁹ temperature (T_V) near 123 K. For many years the accepted model for this order-disorder transition was due to Verwey who proposed that the extra electrons at the iron ions were ordered below the transition temperature in alternate (001) planes of Fe^{2+} and Fe^{3+} ions resulting in an orthorhombic structure. More recent studies,¹⁰ however, have shown that the structure is more

complicated and in fact may be rhombohedral below T_V . Additionally, there exists disagreement among researchers as to the physical mechanism responsible for electrical conduction in magnetite.^{10,11} Several models have been proposed:¹⁰ for example, small polaron hopping,¹² pair localization,¹³ and energy-band schemes.^{11,14} Utilization of different experimental techniques seems to lead researchers to divergent conclusions regarding the conduction mechanism. Thus it is readily apparent that although magnetite has received considerable experimental and theoretical attention, additional work is needed to help clarify the aforementioned points. Therefore we have investigated magnetite by means of μ SR, the main thrust being to ascertain the muon relaxation rate and frequency as a function of temperature with particular attention being paid to the temperature interval encompassing the Verwey transition.

In the course of this study an anomalous change in local field and depolarization rate was observed near 250 K, which is a characteristic of magnetite itself. Although the exact mechanism responsible for this anomaly is not understood at this time it may be correlated with the dynamics of the conduction process in magnetite.

II. EXPERIMENTAL

μ SR experiments¹⁵ on a synthetic single-crystal magnetite sample were performed at the stopped muon channel of the Clinton P. Anderson Meson Physics Facility (LAMPF). Measurements at and below room temperature (RT) were accomplished by using a continuous-flow liquid-helium cryotip with carbon-glass resistance thermometry and a temperature controller. Above RT, sam-

ple heating was provided by a flow of hot nitrogen gas over the crystal with an iron-doped gold versus chromel thermocouple as a sensor. Muon relaxation rates and frequencies were measured as a function of temperature in zero external field. To determine the direction of the magnetic field at the muon site, transverse external field measurements were conducted at RT and 210 K for three different crystallographic directions and applied fields up to 5 kOe. Typically, 10^6 muon decay events were recorded for each data point.

III. RESULTS

In a μ SR experiment one measures the μ^+ polarization at the time of its decay. Superimposed upon the natural μ^+ decay pattern ($\tau_\mu = 2.20 \mu\text{sec}$) is the Larmor precession signal due to the local field at the μ^+ site (\mathbf{B}_μ). For various magnetic materials in zero applied field, it has been shown that \mathbf{B}_μ is given by^{16,17}

$$\mathbf{B}_\mu = \mathbf{B}_{\text{int}} = \mathbf{B}_{\text{dip}} + \mathbf{B}_{\text{hpf}}, \quad (1)$$

where \mathbf{B}_{int} is the total internal field, \mathbf{B}_{dip} is the dipole field, and \mathbf{B}_{hpf} is the hyperfine (Fermi contact) field due to the nonzero electron-spin density at the μ^+ site. In magnetic materials \mathbf{B}_μ is typically large (\sim kOe) which causes the muon-spin polarization to precess at a definite frequency. The μ SR spectrum has the form^{2,16}

$$N(t) = N_0 \exp(-t/\tau_\mu) [1 + P(t)a_0 \cos(2\pi\nu t + \phi)] + \text{const.}, \quad (2)$$

where $P(t)$ is the polarization function, ν is the precession frequency (for free μ^+ the gyromagnetic ratio is 13.55 kHz/Oe), and the constant represents the background events. For our situation $P(t)$ is given by $\exp(-\lambda t)$ with λ being the relaxation or depolarization rate. To obtain a numerical value for the precession frequencies, the modulation spectra $P(t)a_0 \cos(2\pi\nu t + \phi)$ are Fourier analyzed.

Results of a zero-field μ SR experiment on magnetite are given in Fig. 1. The sample was mounted so that the μ^+ beam was perpendicular to the $\langle 111 \rangle$ axis, which, above T_V , is the easy magnetization axis, i.e., the magnetic moments of the iron ions align along this direction.¹⁸ In the temperature region measured, the frequency, and thus the local field, generally follows the bulk magnetization,¹⁹ although there is an abrupt frequency change near 250 K and also at T_V . Detailed frequency measurements were made in this interval ($T_V - \text{RT}$) and are shown in Fig. 2. It should be noted that the discontinuity at T_V is reversed with equal magnitude at 247 K.

To determine the magnitude and direction of the effective local field \mathbf{B}_μ , frequency measurements were made at RT and 210 K as a function of external field. Results for the case where \mathbf{B}_{ext} was applied parallel to the $\langle 110 \rangle$ axis at RT are given in Fig. 3. Similar results were obtained for \mathbf{B}_{ext} parallel to the $\langle 111 \rangle$ and $\langle 100 \rangle$ axes at RT. Of particular interest is the observed splitting of the frequency signal for applied fields larger than ~ 1 kOe at RT (this fact will be considered in the discussion section). This effect is less prominent at 210 K than at RT.

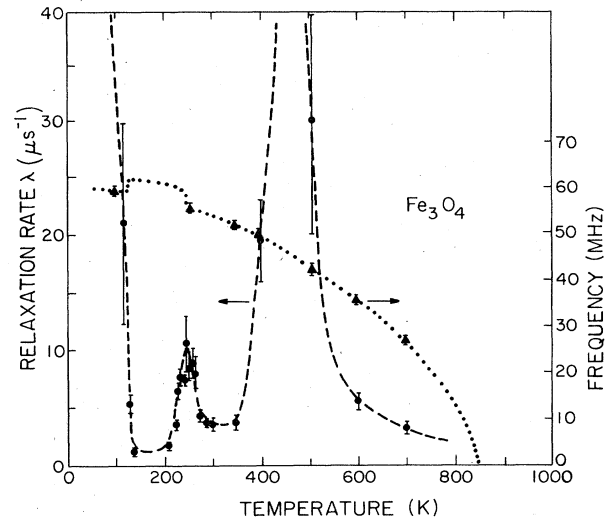


FIG. 1. Temperature dependence of the frequency and relaxation rate of μ SR signals observed in magnetite single crystals at zero applied field. Detailed μ SR measurements for the temperature interval [T_V , RT] are depicted in Fig. 2.

To interpret the data of Fig. 3 it is necessary to calculate \mathbf{B}_μ which must include all the known contributions to the total magnetic energy within a magnetic domain.^{16,20} The relevant magnetic energies are demagnetization (E_{dem}), anisotropy (E_{aniso}), and domain energy due to the external field (E_{ext}); these can be written as

$$\begin{aligned} E_{\text{dem}} &= -\frac{1}{2}NM^2, \\ E_{\text{aniso}} &= -K_1 \sin^2\theta, \\ E_{\text{ext}} &= -\mathbf{M} \cdot \mathbf{B}_{\text{ext}}. \end{aligned} \quad (3)$$

For E_{dem} , N is the sample shape-dependent demagnetization constant and M is the bulk magnetization. The anisotropy energy arises from the spin-orbit interaction at the magnetic ion site. For a spin direction θ with respect

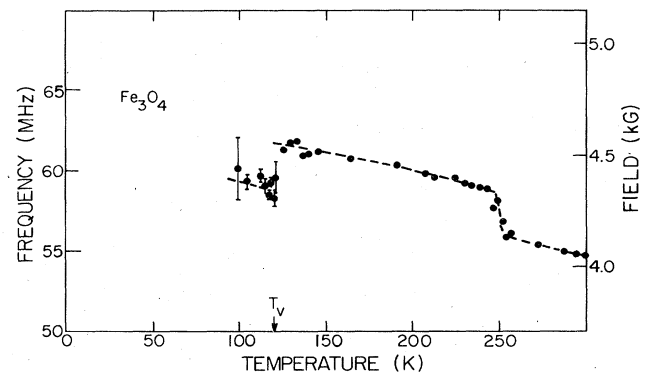


FIG. 2. Muon hyperfine frequencies observed in magnetite in the Verwey-phase-transition temperature region. [About one-half of the data points shown have been measured earlier at the Swiss Institute for Nuclear Research (SIN) and were reported in *Philos. Mag. B* 42, 409 (1980).]

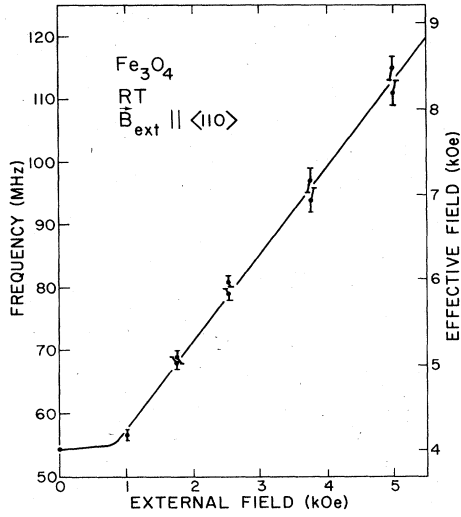


FIG. 3. External field dependence of the μ SR frequency observed in magnetite. The direction of the applied field is parallel to the $\langle 110 \rangle$ axis. The upper signals correspond to a local field larger than the maximum allowable vectorial sum of all the magnetic field contributions (see text for discussion).

to the easy axis of magnetization, the energy in a ferromagnet takes the form $\sum_n K_n \sin^{2n}\theta$; K_1 is the anisotropy constant and is the dominant term in yielding the strength of the interaction.

To interpret the μ SR data for magnetite when an external field is applied, we will treat the system as a ferromagnet (although it is ferrimagnetic), the justification being that the exchange energies are much larger than the weak magnetic anisotropy energy. Shown in Fig. 4 are the per-

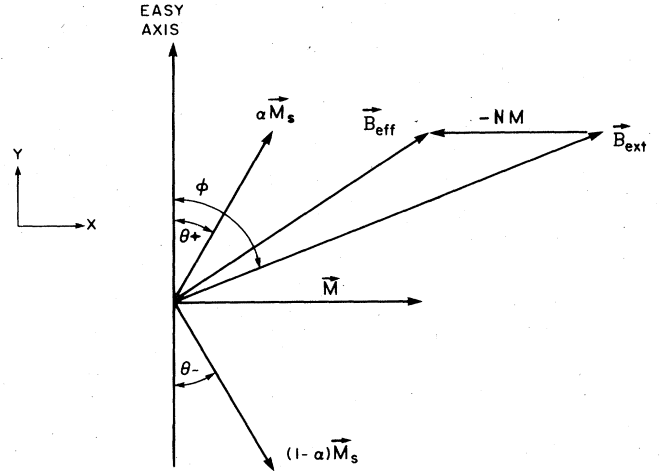


FIG. 4. Magnetic fields and magnetizations present in a ferromagnetic system in an external field which are used for interpretation of the external field (\mathbf{B}_{ext}) dependence Fe_3O_4 data. The effective field (\mathbf{B}_{eff}) is given by $\mathbf{B}_{\text{eff}} = \mathbf{B}_{\text{ext}} - N\mathbf{M}$. The magnetization (\mathbf{M}) is the vector sum of $\alpha\mathbf{M}_s$ and $(1-\alpha)\mathbf{M}_s$ of the two possible domains oriented parallel to the easy axis. For more details see text.

inent magnetic fields for magnetite when an external field is applied. We assume that α is the fraction of domains parallel to the easy magnetization axis (above T_V this is the $\langle 111 \rangle$ axis), M_s is the saturation magnetization of a domain, θ_+ and θ_- are the angles of the domain magnetization with respect to the easy axis, ϕ is the angle of the \mathbf{B}_{ext} direction with the easy axis, and \mathbf{B}_{eff} is the effective applied magnetic field. For the total energy E_{tot} , we may write

$$E_{\text{tot}} = \alpha K_1 \sin^2\theta_+ + (1-\alpha)K_1 \sin^2\theta_- - \alpha B_{\text{ext}} M_s \cos(\phi - \theta_+) + B_{\text{ext}} M_s (1-\alpha) \cos(\phi + \theta_-) + \frac{1}{2} N \{ [\alpha M_s \sin\theta_+ + (1-\alpha) M_s \sin\theta_-]^2 + [\alpha M_s \cos\theta_+ - (1-\alpha) M_s \cos\theta_-]^2 \}. \quad (4)$$

The equilibrium conditions, $dE_{\text{tot}}/d\theta_+ = dE_{\text{tot}}/d\theta_- = dE_{\text{tot}}/d\alpha = 0$, yield $\theta = \theta_+ = \theta_-$. Defining $k_s = 2K_1/NM_s$ and $\mathbf{b}_{\text{ext}} = \mathbf{B}_{\text{ext}}/NM_s$, which are dimensionless parameters, one can show that for equilibrium the following equation is valid,

$$\sin\theta \cos\theta [\alpha k_s + 2\alpha(1-\alpha)] - \alpha b_{\text{ext}} \sin(\phi - \theta) = 0. \quad (5)$$

where $b_{\text{ext}} = |\mathbf{b}_{\text{ext}}|$. We note that when $\phi' = \pi - \phi$, then $\theta' = \theta$ and $\alpha' = 1 - \alpha$. Making use of this fact, we can also write

$$\sin\theta \cos\theta [(1-\alpha)k_s + 2\alpha(1-\alpha)] - (1-\alpha)b_{\text{ext}} \sin(\phi + \theta) = 0. \quad (5')$$

By defining $\beta = 2\alpha - 1$ we can summarize the solution of these equations. For $-1 < \beta < 1$ we have

$$\beta \cos\theta = b_{\text{ext}} \cos\phi, \quad (6)$$

$$(k_s + 1) \sin\theta = b_{\text{ext}} \sin\phi.$$

For $|\beta| = 1$ we have

$$k_s \sin\theta \cos\theta = b_{\text{ext}} \sin(\phi - \theta). \quad (7)$$

A fit to the experimental transverse field data was obtained by using Eqs. (6), (7) (these equations determine θ), and the following equations. For $|\mathbf{b}_{\text{ext}}| < 1$ (or $|\mathbf{B}_{\text{ext}}| < |NM_s|$),

$$B_\mu^2 = [B_{\text{ext}} \sin\phi - NM_s \sin\theta + B_{x \text{ int}}(\theta)]^2 + [B_{y \text{ int}}(\theta)]^2 + [B_{z \text{ int}}(\theta)]^2, \quad (8)$$

and for $|\mathbf{b}_{\text{ext}}| \geq 1$,

$$B_\mu^2 = [B_{\text{ext}} \sin\phi - NM_s \sin\theta + B_{x \text{ int}}(\theta)]^2 + [B_{\text{ext}} \cos\phi - NM_s \cos\theta + B_{y \text{ int}}(\theta)]^2 + [B_{z \text{ int}}(\theta)]^2. \quad (9)$$

We note that in (8) the y component of the demagnetization field ($B_{y\text{dem}}$) cancels $B_{y\text{ext}}$ exactly, as is easily shown by using (6). Taking experimentally known²⁰ values for $K_1(1.1 \times 10^5 \text{ erg/cm}^3)$ and $M_s(500 \text{ Oe})$, the field-dependent μSR data (neglecting the splitting) were fitted with \mathbf{B}_{int} and N as free parameters. The results of this fit are shown as the solid line in Fig. 3. Similar fits were also obtained for the other crystal orientations. The observed demagnetization fields are of the order of 1 kOe which is in reasonable agreement with the calculated value for the sample geometry.²⁰ Furthermore, we find that for external fields weaker than the demagnetization field, the internal field rotates from the $\langle 111 \rangle$ axis to the \mathbf{B}_{ext} direction as \mathbf{B}_{ext} increases, and also that when the external field is stronger than \mathbf{B}_{dem} , \mathbf{B}_{int} is parallel to \mathbf{B}_{ext} . These fits to the data sets based upon the preceding analysis are consistent with an internal field parallel to the $\langle 111 \rangle$ axis in zero applied field. The internal field at RT for magnetite is 4.02 kOe in agreement with the zero applied field measurements.

IV. DISCUSSION

The data, particularly at and above RT, appear to be consistent with those from other magnetic oxides^{3,6-8} where (1) the direction of the observed field is in the direction of the magnetization, (2) the temperature of the local field follows the magnetization curve, and (3) a maximum in the relaxation rate occurs between 400 and 500 K. These data were interpreted in terms of muon motion (localization and local or global diffusion) and changes in the local field experienced by the muon.

As shown in Fig. 1 the muon relaxation rate in magnetite increases dramatically as T_V is approached from higher temperatures; moreover, there exists a corresponding abrupt change in the muon hyperfine frequency associated with the local field. These results are to be expected if one invokes the model of hopping electrons between the octahedral iron sites, which ceases at T_V with a simultaneous structural phase transition producing a different magnetic environment for the muon.

Conversely, there is no abrupt change in the frequency near 400 and 500 K that corresponds to the drastic change in relaxation rate. This behavior is a manifestation of muon motion as opposed to magnetic or structural changes associated with the local field. At temperatures above 700 K the muon diffuses quite rapidly throughout the entire lattice and is "motionally narrowed" due to relatively large variations of \mathbf{B}_{dip} , while it samples many sites. As the temperature is lowered from 700 K the muon begins to slow down and consequently samples appreciably fewer sites, thereby producing a measurable relaxation rate; the muon is still undergoing global diffusion but at a slower rate. With a further decrease in temperature (400–150 K) the muon motion will be confined to a local region of the lattice. This local diffusion will cause a decrease in the muon relaxation rate as observed near 400 K.

At RT Rüegg *et al.*⁶ have used similar arguments to explain the relaxation data in $\alpha\text{-Fe}_2\text{O}_3$. Vanishing of the μSR signal between 500 and 750 K led them to conclude

that the muon was no longer localized, and, in fact, hopped from sites with the field in a positive direction to sites with the same magnitude field in the opposite direction (recall that Fe_2O_3 is antiferromagnetic). This model was substantiated by data above 650 K, where the average internal field was zero; yet, the muon precession signal could be restored by applying an external field.

The origin of the local-field discontinuity and relative maximum in relaxation rate at 247 K is not understood at this time. As we have reported earlier,²¹ the anomaly is not due to a change in the muon state but is associated with magnetite and may be a precursor of the Verwey phase transition. An anomaly in the magnetic permeability at nearly the same temperature has recently been found;²² however, the features appear to be different. For example the μSR anomaly does not show a temperature hysteresis in contrast to the reported results. Based upon our previous reasoning, we would argue that it corresponds to a magnetic transition somewhat analogous to that observed at T_V .

There are known¹⁰ dynamic processes occurring in magnetite in this temperature regime which may provide insight into our current observations. The current model of conduction mechanism for magnetite above T_V is phonon-assisted electron hopping along the $\text{Fe}^{2+}\text{-Fe}^{3+}$ cation chains in the B sublattice. Furthermore, it is highly probable that electron-phonon interactions are key factors in establishing Verwey order. Above T_V correlated atomic group motion (molecular polarons) is observed via neutron scattering experiments.²³ These polarons affect the electron hop time and may well provide a different magnetic environment for the muon. One possibility is cross relaxation between the muon precession frequency and the time-modulated magnetic environment.

From Mössbauer measurements²⁴ it is calculated, using the method of Kündig *et al.*,²⁵ but correcting for an existing quadrupole effect,²⁴ that the electron hop time near 250 K is $3(\pm 1)$ ns. From our μSR data we find that the frequency associated with the local maximum relaxation rate at 247 K is 57.5 MHz. Efficient cross relaxation occurs when $\omega\tau \approx 1$, from whence one can calculate $\tau_{\text{hop}} = 1/2\pi\nu$, where $\nu = 57.5$ MHz. This yields an electron hop time of 2.8 ns. Such remarkable agreement between the hop times may be fortuitous, or, alternatively, may indicate that μSR can probe the time dependence of dynamic behavior associated with the local magnetic environment.

At external fields greater than ~ 1 kOe, a splitting is present, which appears to be proportional to the $|\mathbf{B}_{\text{ext}} - \mathbf{B}_{\text{dem}}|$ and seems to be crystal-orientation dependent.²¹ The previously discussed formalism cannot explain this phenomena; in fact, the upper set of frequency signals (see Fig. 3) corresponds to magnetic fields larger than the maximum possible vectorial sum of all the fields. Slight crystal misalignments, multiple crystal grains, or a distortion of the iron spin system cannot cause these features of the anomalous splitting.

The data upon which the splitting is based does not yield two clearly resolved frequencies; however, attempts to fit the time spectra with a single frequency and exponential relaxation give nonphysical results. For exam-

ple, a forced fit to the data for $B_{\text{ext}}||\langle 110 \rangle$ at 5 kOe yields the following unreasonable parameters: $a_0=0.31 (\pm 0.07)$, $\lambda=10.9 (\pm 1.4) \mu\text{s}^{-1}$, and a "forbidden" high frequency of $\nu=114.1 (\pm 0.2) \text{MHz}$. The beat pattern, which one should observe if two frequencies are present, is difficult to see because the beat frequency and the muon depolarization rate at zero applied field are of the same order of magnitude. This is also the cause of the excessively high asymmetry and depolarization rate in the forced fit.

Due to the large errors the magnitude of the splitting with respect to external field has not been determined accurately enough to elucidate the functional relationship of the two; i.e., we do not know if the splitting is linear, quadratic, etc. with external field. Such information is necessary before one can formulate a model to explain the phenomenon. However, one might speculate that there is a connection between the anomaly observed at 247 K and the anomalous broadening (splitting) in applied fields at RT. If our cross-relaxation interpretation is correct, an external field would shift the anomaly to higher temperatures. This experiment is planned for the future.

As stated previously, it appears that the muon behavior in magnetite is similar to other magnetic oxides. Thus, questions arise as to the set of sites the muon hops into and to the origin of the observed magnetic field. For the antiferromagnetic corundum-structured oxides⁷ two sets of muon sites have been found for which the local field must be of both hyperfine and dipolar nature [see formula (1)]. In the case of the rare-earth orthoferrites it is possible to identify the muon site on the basis of point-dipole contributions alone⁸ due to the fact that the hyperfine field at the favored sites is zero to first order.²⁶ For example, ErFeO_3 exhibits a spin rotation near 100 K and the dipole fields for both spin orientations can be calculated. A favorable site is found in which the calculation agrees with the observed field both in magnitude and direction for each spin orientation with the muon residing 1 Å away from the oxygen ion. Several researchers²⁷ have suggested that this localization of the muon corresponds to a muon-oxygen bond analogous to a hydrogen bond.

Presently, the muon stopping site for magnetite has not been unequivocally located; however, recent preliminary hyperfine-field calculations²⁸ have shown that it is quite likely that the muon localizes at a site structurally similar to those reported for hematite (Fe_2O_3) where muon-oxygen bond formation was suggested. The hyperfine-field calculations were based upon three experimental facts: (1) the magnitude of B_{int} must be 4.02 kOe at RT; (2) in zero applied field B_{int} is parallel to the $\langle 111 \rangle$ direction; and (3) when the external field exceeds B_{dem} , B_{μ} must be in the B_{ext} direction. Conditions (2) and (3) suggest that B_{int} is parallel to the iron magnetic moments for all crystal orientations with respect to B_{ext} , a characteristic of a hyperfine field rather than a pure dipolar one. The origin of this field can be the muon-oxygen bond where the muon 1s orbital overlaps the oxygen 2p orbital which, in turn, transfers an electron to an unoccupied 3d orbital of the iron ions. Such a situation would produce covalency effects which are the cause of a so-called supertransfer hyperfine field.^{7,26}

On the other hand, muon sites can be found,²⁸ where in zero applied field, B_{dip} is parallel to the $\langle 111 \rangle$ axis and its magnitude equals 4.0 kOe; in this case, however, condition (3) is not fulfilled. When B_{ext} changes direction, B_{dip} changes its direction quite differently. The iron spins themselves will reorient parallel to the applied field; however, the resulting dipole field at any site will in most cases not be parallel to this direction. This objection also applies to the sites found in similar calculations,³ where the assumption was made that the muon diffuses rapidly among nearby oxygens. Electrostatically favorable sites were found for which the dipolar component along the $\langle 111 \rangle$ axis in zero applied field can be 4.0 kOe and the perpendicular components are averaged to zero due to rapid local muon motion.

In the above-mentioned calculations²⁸ an approximate method was also used to incorporate local muon motion, the dipolar field components parallel to the iron spins were required to be approximately equal for the spin directions $\langle 111 \rangle$, $\langle 110 \rangle$, and $\langle 100 \rangle$. A further requirement, viz., that muon motion among a set of neighboring sites should produce average perpendicular components of zero, was used to place additional restrictions on the site search. This search algorithm as well as the other somewhat different algorithms generated six so-called Rüegg sites within an octahedron of oxygens and between two iron A-site ions along the $\langle 111 \rangle$ axis.^{3,28} These sites are similar to the Rodriguez sites found in hematite.^{5,7} We note that based on potential-energy considerations the muon should reside in regions similar in symmetry and environment to that in $\alpha\text{-Fe}_2\text{O}_3$, for which the Rodriguez sites were reported.

The magnitude of the motional-averaged dipolar component is about 5 kOe.²⁸ To explain the measured field using Eq. (1), the supertransfer hyperfine field must be 1 or 9 kOe because B_{μ} is either parallel or antiparallel with respect to B_{dip} . For the Rodriguez sites in $\alpha\text{-Fe}_2\text{O}_3$ the following field contributions were found⁵ to have opposite directions: $B_{\text{dip}}=20.7 \text{ kOe}$ and $B_{\text{sthf}}=4 \text{ kOe}$. Assuming the muon is localized in a similar magnetic environment and, accordingly, applying the same ratio $B_{\text{sthf}}/B_{\text{dip}}$ for magnetite one obtains $B_{\text{sthf}}=1 \text{ kOe}$ for the Rüegg sites. This indicates that for these sites in magnetite the muon hyperfine field is mainly of dipolar nature, but a supertransfer term is also needed to interpret the data. Potential-energy calculations must be performed to confirm the Rüegg sites in magnetite and produce possible diffusion paths such that refined hyperfine-field calculations can provide support in this search for possible muon stopping sites in magnetite.

In conclusion, we have presented data depicting positive-muon behavior in magnetite. The internal field is 4.02 kOe and is parallel to the iron magnetic moments ($\langle 111 \rangle$ direction at RT), i.e., the easy axis of magnetization. The origin of the internal field is not completely established at this time, but it appears that a muon-oxygen bond is formed in the same way as reported for other magnetic oxides. In addition to a dominant dipolar contribution, a supertransfer hyperfine-field term is necessary to account for the internal field observed in magnetite. Anomalies in the muon hyperfine interactions have been

observed at 247 K in zero applied field and at RT in applied fields larger than the demagnetization field. The underlying mechanisms for these anomalies may be associated with the dynamics of the phonon-assisted electron conduction process. Further detailed studies may show that the 247 K anomaly is a precursor of the Verwey phase transition in magnetite.

ACKNOWLEDGMENTS

The authors gratefully acknowledge the assistance of C. E. Olsen of Los Alamos for his work in the x-ray analysis and orientation of the magnetite crystals used in this investigation. With pleasure we acknowledge the staff of

the Clinton P. Anderson Meson Physics Facility (LAMPF, Los Alamos) for providing the experimental area and beam support. The first μ SR measurements on magnetite were performed at the Swiss Institute for Nuclear Research. Two of the authors (C. B. and A. B. D.) acknowledge the assistance and collaboration of the μ SR workers at the Physik Institute, University of Zürich, Zürich, Switzerland. We would like to thank especially Dr. Kurt J. Rüegg for his valuable contributions to the muon-spin research in magnetic oxides. The research at Los Alamos is supported by the U. S. Department of Energy; the research at Texas Tech is supported by the Robert A. Welch Foundation. Two of the authors (C. B. and V. A. M. B.) acknowledge a NATO travel grant.

¹Third International Conference on Muon Spin Rotation, Shimoda, Japan, 1983 [Hyperfine Interact. 15-17 (1984)].

²E. Karlsson, Phys. Rep. 82 (5), 272 (1982).

³A. B. Denison, J. Appl. Phys. 55, 2278 (1984).

⁴K. J. Rüegg, C. Boekema, A. B. Denison, W. P. Hofmann, and W. Kündig, J. Magn. Magn. Mater. 15-18, 669 (1980).

⁵C. Boekema, K. J. Rüegg, and W. P. Hofmann, Hyperfine Interact. 8, 609 (1981).

⁶K. J. Rüegg, C. Boekema, W. Kündig, P. F. Meier, and B. D. Patterson, Hyperfine Interact. 8, 547 (1981).

⁷C. Boekema, A. B. Denison, and K. J. Rüegg, J. Magn. Magn. Mater. 36, 111 (1983).

⁸E. Holzschuh, A. B. Denison, W. Kündig, P. F. Meier, and B. D. Patterson, Phys. Rev. B 27, 5294 (1983).

⁹E. J. W. Verwey and P. W. Haayman, Physica (Utrecht) 8, 979 (1941).

¹⁰A. J. M. Kuipers and V. A. M. Brabers, Phys. Rev. B 14, 1401 (1976). See also *Proceedings of the International Meeting on Magnetite and Other Materials Showing a Verwey Transition, Cambridge 1979* [Philos. Mag. B 42 (1980)]. For two excellent reviews see N. F. Mott, *Metal-Insulator Transitions* (Taylor and Francis, London, 1974), and J. M. Honig, J. Solid State Chem. 45, 1 (1982).

¹¹A. J. M. Kuipers and V. A. M. Brabers, Phys. Rev. B 20, 594 (1979).

¹²D. L. Camphausen, Solid State Commun. 11, 99 (1972).

¹³U. Buchenau, Solid State Commun. 11, 1287 (1972).

¹⁴J. R. Cullen and E. Callen, Phys. Rev. Lett. 26, 236 (1971);

Phys. Rev. B 7, 397 (1973).

¹⁵For a description of our spectrometer, see C. Boekema, R. H. Heffner, R. L. Hutson, M. Leon, M. E. Schillaci, W. J. Kossler, M. Numan, and S. A. Dodds, Phys. Rev. B 26, 2341 (1982).

¹⁶A. B. Denison, H. Graf, W. Kündig, and P. F. Meier, Helv. Phys. Acta. 52, 460 (1979).

¹⁷P. F. Meier, Hyperfine Interact. 8, 591 (1981).

¹⁸L. R. Bickford, Phys. Rev. 76, 137 (1949).

¹⁹R. S. Tebble and D. J. Craik, *Magnetic Materials* (Wiley-Interscience, New York, 1969), Chap. 7.

²⁰A. H. Morrish, *The Physical Principles of Magnetism* (Wiley, New York, 1965).

²¹C. Boekema, V.A.M. Brabers, A. B. Denison, R. H. Heffner, R. L. Hutson, M. Leon, C. E. Olsen, and M. E. Schillaci, J. Magn. Magn. Mater. 31-34, 709 (1983).

²²J. M. Honig and R. Aragon (private communication).

²³Y. Yamada, N. Wakabayashi, and R. M. Nicklow, Phys. Rev. B 21, 4642 (1980).

²⁴C. Boekema, J. de Jong, F. van der Woude, and G. A. Sawatzky, Physica 86-88B, 948 (1977).

²⁵W. Kündig and R. S. Hargrove, Solid State Commun. 7, 223 (1969).

²⁶C. Boekema, Hyperfine Interact. 17-19, 305 (1984).

²⁷References 3, 7, 8, and 26, and references therein.

²⁸C. Boekema, A. B. Denison, D. W. Cooke, R. H. Heffner, R. L. Hutson, M. Leon, and M. E. Schillaci, Hyperfine Interact. 15-16, 529 (1983).